

Unconditional Microwave Quantum Teleportation of Gaussian States in Lossy Environments

Vahid Salari

Department of Physical Chemistry, University of the Basque Country UPV/EHU, Apdo. 644, 48080 Bilbao, Spain

(Dated: March 5, 2021)

Here, a physical formalism is proposed for an unconditional microwave quantum teleportation of Gaussian states via two-mode squeezed states in lossy environments. The proposed formalism is controllable to be used in both the fridge and free space in case of entanglement between two parties survives. Some possible experimental parameters are estimated for the teleportation of microwave signals with a frequency of 5GHz based on the proposed physical framework. This would be helpful for superconducting inter- and intra-fridge quantum communication as well as open-air quantum microwave communication, which can be applied to quantum local area networks (QLANs) and distributed quantum computing protocols.

Introduction— In recent years, several achievements have been reported [1–6], which are now the potential building blocks of microwave quantum communication protocols. This novel research area is not only useful for free space communications, but also a candidate for chip-to-chip communication, required by distributed quantum computing. The latter represents an alternative paradigm to increasing the number of qubits in a single quantum processor, and aims at solving larger quantum algorithms in a distributed form between different processors with lower number of qubits. Nowadays, one of the best quantum platforms suited for quantum computing is superconducting circuits, which interact via microwave photons. The main challenge concerns the efficient distribution of such microwave states between circuits, the two main options being direct state transfer and teleportation. Concerning the former, several experiments have been done in a single cryogenic environment [7–13], as well as with microwave to optical conversion [14, 15]. Recently, a successful transfer of transmon qubits has been reported, via a cryogenic waveguide coherently linking two dilution refrigerators separated by five meters, with average transfer and target state fidelities of 85.8 % and 79.5 %, respectively, in terms of discrete variables [16].

So far, microwave teleportation between two fridges has not been investigated experimentally, neither in terms of discrete variables nor continuous variables (CVs). However, a teleportation scheme in the microwave regime in terms of CVs has been proposed before [17]. Taking into account the limitations of the previous protocol, we investigate the feasibility of an experimental implementation of microwave quantum teleportation of Gaussian states in real conditions, e.g. fridge and free space, in terms of CVs based on a clear physical formalism. Indeed, in quantum information processing with CVs, Gaussian states play important roles [19, 21], which are well-known and commonly-used experimentally. Here, we focus on teleportation of single-mode Gaussian states via entangled two-mode Gaussian states.

Quantum Teleportation with CVs—A preliminary CV model for teleportation was proposed by Vaidman [23], and then developed by Braunstein and Kim-

ble [24]. The latter represented a conditional teleportation protocol, whereas an unconditional one was proposed by Furusawa et al. [25].

Quantum teleportation uses quantum entanglement and classical communication to transfer quantum information between two distant parties, Alice and Bob. The ideal scenario involves Alice and Bob sharing a maximally-entangled state, which in CVs translates to a two-mode squeezed vacuum (TMSV) state with infinite squeezing r . In a realistic scenario, the squeezing r has technological limitations. In such protocol, Alice attempts to send a Gaussian state, with covariance matrix V'_{in} and first moments $\bar{x}'_{\text{in}} = (x_{\text{in}}, p_{\text{in}})$ (see Appendix) to Bob. The input state can also be described by a harmonic oscillator mode $\alpha_{\text{in}} = \frac{x_{\text{in}} + ip_{\text{in}}}{\sqrt{2}}$. If this process is successful, then Alice and Bob share a Gaussian entangled state with covariance matrix V_{TMS} and null first moments [22]. Then, after entangling the input state with TMS, Alice makes a double homodyne measurement of both quadratures (i.e. a heterodyne detection) and modulates the classical results, X_u and P_v , in the form of a single mode $\delta = \frac{X_u + iP_v}{\sqrt{2}}$ and then sends it to Bob. Finally, Bob applies a unitary displacement with a function of δ to his share of the original entangled state to reconstruct the input state (see Fig. 1). Different teleportation protocols in terms of CVs are discussed in Ref. [26]. In the following, we focus basically on the Braunstein-Kimble protocol [24] for teleportation of Gaussian states.

Measurement by Alice—When Alice receives the mixture of input mode and one mode of the entangled state, she performs a double homodyne detection (see Fig. 2), which is the optimal measurement for the teleportation protocol. In this case, the results of the measurement (which are two classical values, X_u and P_v) will be modulated as a single mode δ to be sent to Bob. As seen in Fig. 2, two modes α_{in} and α_1 are passing through a 50:50 beamsplitter, and then again each output beam again passes through two other 50:50 beamsplitters while a classical local oscillator mode α_{LO_e} enters in the top beamsplitter and another classical local oscillator mode α_{LO_p} passes through the other beamsplitter. According

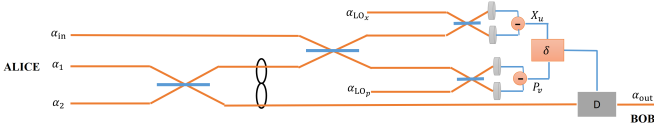


FIG. 1. The Braunstein-Kimble Protocol for the Teleportation of Gaussian States. In this protocol, two parties, Alice and Bob, share an entangled quantum state with two modes α_1 and α_2 . In fact, Alice wants to send a single-mode Gaussian state (i.e. mode α_{in}) to Bob via the teleportation mechanism where she cannot send the original mode α_{in} to Bob directly but a classical mode δ is sent instead. Finally, Bob can reconstruct the input state by applying the displacement $D(\delta)$ operator on his mode α_2 to construct the input state as $\alpha_{\text{out}} \approx \alpha_{\text{in}}$.

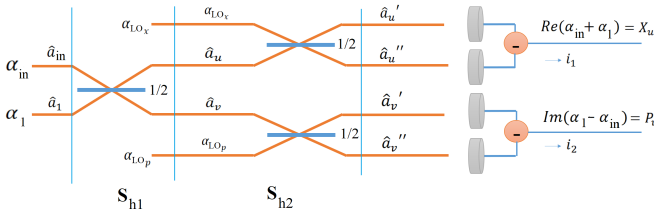


FIG. 2. Alice's measurement is performed via double homodyne detection. First, two modes α_{in} and α_1 passing through a 50:50 beamsplitter, and then again each output beam again passes through two other 50:50 beamsplitters while a classical local oscillator mode α_{LO_x} enters in the top beamsplitter and another classical local oscillator mode α_{LO_p} passes through the other beamsplitter. Then, Alice performs a double homodyne detection where the classical result of the measurement will be modulated as a single mode δ to be sent to Bob.

to Fig. 2 in each line for quantum modes we use the annihilation operators, and α as classical coherent state for the local oscillator. Finally, there would be four outputs at the end, where there is a detector at each output which can measure the current produced due to the collision of photons to the detector.

In the symplectic representation (see Appendix), we consider two symplectic operators in the double-homodyne detection circuit depicted in Fig. 2, $S_{h1} = \mathbb{I}_2 \oplus B_S(1/2)_4 \oplus \mathbb{I}_2$ and $S_{h2} = B_S(1/2)_4 \oplus B_S(1/2)_4$ where \mathbb{I}_2 is the identity 2×2 matrix, and $B_S(1/2)_4$ is the 50:50 beamsplitter operator, i.e. a 4×4 matrix. The input first moment in the double-homodyne detection is $\bar{\mathbf{x}}'_{\text{in}} = (x_{\text{LO}_x}, p_{\text{LO}_x}, x_{\text{in}}, p_{\text{in}}, e^r x_1, e^{-r} p_1, x_{\text{LO}_p}, p_{\text{LO}_p})^T$, and therefore the output's first moments at the photodetectors right before the measurement are $\bar{\mathbf{x}}'_{\text{out}} = S_{h2} S_{h1} \bar{\mathbf{x}}'_{\text{in}}$, which gives $\bar{\mathbf{x}}'_{\text{out}} = \sqrt{2}((x_{u'}, p_{u'}), (x_{u''}, p_{u''}), (x_{v'}, p_{v'}), (x_{v''}, p_{v''}))^T$.

Here, we assume that the detectors are ideal, therefore we define the produced current as $i = \langle \hat{n} \rangle = \langle \hat{a}^\dagger \hat{a} \rangle = \langle 1/2(\hat{x}^2 + \hat{p}^2) - 1/2 \rangle = 1/2(x^2 + p^2) - 1/2$. Then, the difference between the currents from each detector after the beam splitters is measured [27]. The current from the

top beamsplitter is the difference between the currents in u' and u'' , i.e. $i_1 = \langle \hat{a}_{u'}^\dagger \hat{a}_{u'} \rangle - \langle \hat{a}_{u''}^\dagger \hat{a}_{u''} \rangle$, and in the other two arms $i_2 = \langle \hat{a}_{v'}^\dagger \hat{a}_{v'} \rangle - \langle \hat{a}_{v''}^\dagger \hat{a}_{v''} \rangle$. Assuming $\alpha_{\text{LO}_x} = |\alpha_{\text{LO}_x}\rangle e^{i\theta_x}$, one obtains $i_1 = |\alpha_{\text{LO}_x}|(x_{\text{in}} + e^r x_1)$ by letting $\theta_x = 0$ that consequently can obtain $X_u = \frac{i_1}{|\alpha_{\text{LO}_x}|} = x_{\text{in}} + e^r x_1 = \text{Re}(\delta)$. Similarly $\alpha_{\text{LO}_p} = |\alpha_{\text{LO}_p}\rangle e^{i\theta_p}$, if we let $\theta_p = \pi/2$ then it turns to $i_2 = |\alpha_{\text{LO}_p}|(p_{\text{in}} - e^{-r} p_1)$, and therefore $P_v = \frac{i_2}{|\alpha_{\text{LO}_p}|} = p_{\text{in}} - e^{-r} p_1 = \text{Im}(\delta)$. By using classical coherent light with similar amplitudes for both local oscillators, one can write $|\alpha_{\text{LO}_x}| = |\alpha_{\text{LO}_p}| = |\alpha_{\text{LO}}|$, so the currents i_1 and i_2 can be modulated into a single mode as $\delta = X_u + iP_v$, to be sent and received by Bob. On the other side, at the same time that Alice measures her state, the state at Bob collapses to $\alpha_2 = \frac{e^r x_2 + i e^{-r} p_2}{\sqrt{2}}$ with $x_2 = -x_1$ and $p_2 = p_1$. Comparing δ and α_2 we realize that $\delta + \alpha_2 = \alpha_{\text{in}}$. Once Bob receives this information, he can reconstruct Alice's input state by applying the displacement $D(\delta)$ on his mode, i.e. $D(\delta)|\alpha_2\rangle = |\delta + \alpha_2\rangle = |\alpha_{\text{out}}\rangle \approx |\alpha_{\text{in}}\rangle$. In the symplectic representation, this means that the first moments of Bob, $\bar{\mathbf{x}}_2 = (x_2, p_2)^T$ should be displaced with $\Delta = (X_u, P_v)^T$, which means

$$\bar{\mathbf{x}}_2 \rightarrow \bar{\mathbf{x}}_2 + \Delta. \quad (1)$$

The performance of the teleportation protocol can be measured by the teleportation fidelity F . It can be computed via a symplectic approach [20, 26], i.e. $F = 2/\sqrt{\det(\Gamma)}$, in which $\Gamma = 2V'_{\text{in}} + \mathbb{Z}A\mathbb{Z} + B - C\mathbb{Z} - \mathbb{Z}^T C^T$ where A , B , and C are the block matrices of two-mode squeezed states (TMSS) in symplectic representation, i.e. shown by a block matrix as $V_{\text{TMSS}} = [A, C; C^T, B]$, where $A = A^T$, $B = B^T$ and C is a 2×2 real matrix, and T denotes transpose [22]. If the input is a squeezed coherent state, i.e. $V'_{\text{in}} = \begin{pmatrix} e^{2y} & 0 \\ 0 & e^{-2y} \end{pmatrix}$ where y is the squeezing level of the input, the fidelity in general form is obtained as

$$F = \frac{1}{\sqrt{(e^{-2y} + (2n+1)\sigma)(e^{+2y} + (2n+1)\sigma)}}. \quad (2)$$

where $\sigma = \exp(-2r)$ is the variance of the resource, and n is the number of thermal photons in the two-mode squeezed thermal states (TMSTS) resource as a general form for TMSS. The particular case $n = 0$ represents the fidelity for the general case when the resource is TMSV (see Appendix). One can compute the average fidelity for the teleportation of an arbitrary squeezed displaced vacuum state by integration over fidelity in the range 0 and 1.

Microwave Quantum Teleportation— Microwave quantum communication, as an exciting line of research with potentially broad applications in science and industry, is an accessible technology due to the recent achievements of circuit quantum electrodynamics (cQED). Since thermal noise in the microwave domain are much larger than in the optical one, losses have to be taken into account, which can significantly affect the quality of the

teleportation protocol. In order to suppress thermal fluctuations, macroscopic superconducting circuit operate at low temperatures, i.e. $T < 10 - 100\text{mK}$ [17]. In cQED, superconducting Josephson junctions are nonlinear elements which have essential applications in quantum computation and quantum information. Recently, path-entanglement between propagating quantum microwaves as TMSS was generated via Josephson parametric amplifiers (JPAs) and hybrid ring [4] to be used to perform microwave protocol equivalent to the traditional ones in optical quantum teleportation. In this protocol, a TMSS is generated from two single-mode squeezed states, with squeezing in orthogonal quadratures, generated by two JPAs, J_1 and J_2 at the same squeezing level r with possible endogenous thermal photons, and then sending them through a hybrid ring, which is a microwave beam splitter [4, 17]. In general, the quality of the entanglement between the two modes is affected by thermal fluctuations on the JPA during the generation of the single-mode squeezed states. Then, after the interaction of one mode with the input state via 50:50 beamsplitter, the outputs are connected to other two JPAs, J_3 and J_4 , which operate as amplifiers with equal gain $g_J = \exp(2r_J)$ with squeezing parameter r_J (see Fig. 3). The final step is the measurement by Alice via heterodyne detection. The method is the same as what we explained before (and in Appendix) but with taking amplifications and losses into account. Transfer efficiencies are modelled by beamsplitters with reflectivities ϵ , η , κ , and ν , where the losses are indeed $1 - \epsilon$, $1 - \eta$, $1 - \kappa$, and $1 - \nu$, respectively. The reflectivity η represents the interaction of TMSS in free space. Other losses are related to JPAs and amplifiers. For simplicity, we choose $\epsilon_1 = \epsilon$, $\epsilon_2 = 1$, $\eta_1 = \eta$, and $\eta_2 = 1$. If the single-mode operator J_{in} squeezes the input coherent state with squeezing parameter y , e.g. $J_{\text{in}} = [e^{-y}, 0; e^y, 0]$, it produces a squeezed coherent state as $\alpha_{\text{in}} = (e^{-y}x_{\text{in}} + ie^y p_{\text{in}})/\sqrt{2}$, which is the state to be teleported. Following the procedure in heterodyne detection, the output components can be obtained as $X_u = |\alpha_{\text{LO}}| \sqrt{\nu\kappa g_J} [e^{-y}x_{\text{in}} + (e^r x_1 \sqrt{\eta\epsilon} + \zeta_{x_1})] \cos(\theta_x)$ and $P_u = |\alpha_{\text{LO}}| \sqrt{\frac{\nu\kappa}{g_J}} [e^y p_{\text{in}} + (e^{-r} p_1 \sqrt{\eta\epsilon} + \zeta_{p_1})] \sin(\theta_x)$ as the real and imaginary parts, respectively. By letting $\theta_x = 0$ the current i_1 turns to

$$X_u = [|\alpha_{\text{LO}}| (\sqrt{\nu\kappa g_J} (e^r x_1 \sqrt{\eta\epsilon} + e^{-y} x_{\text{in}}) + \zeta_x)] \quad (3)$$

and $P_u = 0$ where ζ_x is the noise term, i.e. $\zeta_x = x_{\text{th-1}} \sqrt{\nu\kappa\eta(1-\epsilon)} + x_{\text{th-2}} \sqrt{\nu\kappa(1-\eta)} + x_{\text{th-3}} \sqrt{\nu(1-\kappa)} + x_{\text{th-4}} \sqrt{1-\nu}$ where $x_{\text{th-}i}$ ($i=1, 2, 3, 4$) are thermal quadratures at temperatures T_1, T_2, T_3 , and T_4 respectively. If there are no losses ($\epsilon = \eta = \kappa = \nu = 1$), then the current is $i_1 = |\alpha_{\text{LO}}| \sqrt{g_J} (e^r x_1 + e^{-y} x_{\text{in}})$. Similarly for current i_2 , one can obtain $X_v = |\alpha_{\text{LO}}| \sqrt{\frac{\nu\kappa}{g_J}} [e^{-y} x_{\text{in}} - (e^r x_1 \sqrt{\eta\epsilon} - \zeta_{x_2})] \cos(\theta_p)$ and $P_v = |\alpha_{\text{LO}}| \sqrt{\nu\kappa g_J} [e^y p_{\text{in}} - (e^{-r} p_1 \sqrt{\eta\epsilon} - \zeta_{p_2})] \sin(\theta_p)$. Again, under similar conditions, but letting

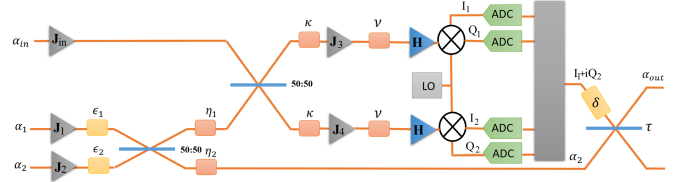


FIG. 3. Microwave quantum teleportation circuit for Gaussian states

$\theta_p = \pi/2$ the current i_2 turns to

$$P_v = |\alpha_{\text{LO}}| [\sqrt{\nu\kappa g_J} (e^y p_{\text{in}} - e^{-r} p_1 \sqrt{\eta\epsilon}) + \zeta_p] \quad (4)$$

and $X_v = 0$, where the noise term ζ_p is $\zeta_p = p_{\text{th-1}} \sqrt{\nu\kappa\eta(1-\epsilon)} + p_{\text{th-2}} \sqrt{\nu\kappa(1-\eta)} + p_{\text{th-3}} \sqrt{\nu(1-\kappa)} + p_{\text{th-4}} \sqrt{1-\nu}$. If there is no any loss, then the noise term turns to zero, and $i_2 = |\alpha_{\text{LO}}| \sqrt{g_J} (e^y p_{\text{in}} - e^{-r} p_1)$.

The above results are in agreement with the heterodyne outputs (see the Appendix) by letting $g_J = 1$ and $y = 0$ for coherent states in the BK protocol. In reality, there are always losses for microwave signals. So, it is desirable to reduce the losses as far as possible to have a successful quantum protocol, otherwise the noisy signal received by Bob makes it harder to reconstruct the input state. In fact, the realization of a microwave single-photon detector is a difficult task due to the low energy of microwave photons, therefore measuring a quadrature of a weak microwave signal is hard. Thus, amplification of the signal is required. Cryogenic high electronic mobility transistor (HEMT) amplifiers are routinely used in quantum microwave experiments because of their large gains in a relatively broad frequency band. Basically, HEMT amplifiers are phase insensitive and add a significant amount of noise photons that may disrupt the protocol (see section E. on Amplification). These signals are digitized with analog-to-digital (ADC) converters and sent to a computer for digital data processing [4]. In terms of ADC in heterodyne detection, quadrature moments are I_1, I_2, Q_1 , and Q_2 (see Fig. 3) which are calculated and averaged in the computer. The I and Q components can be described in terms of continuous variables x and p , so they can be written as $I_i = \sqrt{\hbar\omega_i BR g_H} x_i$ and $Q_i = \sqrt{\hbar\omega_i BR g_H} p_i$, where $R = 50\Omega$, B is the measurement bandwidth set by a digital filter, and g_H is the HEMT gain. The modulated classical signal $\delta = I_1 + iQ_2 = \sqrt{\hbar\omega_i BR g_H} (X_u + iP_v)$ is communicated classically with Bob, where

$$I_1 = \sqrt{\hbar\omega_i BR g_H} [|\alpha_{\text{LO}}| (\sqrt{\nu\kappa g_J} (e^{-y} x_{\text{in}} + \sqrt{\eta\epsilon} e^r x_1 + \zeta'_x))],$$

$$Q_2 = \sqrt{\hbar\omega_i BR g_H} [|\alpha_{\text{LO}}| (\sqrt{\nu\kappa g_J} (e^y p_{\text{in}} - \sqrt{\eta\epsilon} e^{-r} p_1 + \zeta'_p))]$$

where $\zeta'_x = \frac{\zeta_x}{\sqrt{\nu\kappa g_J}}$, and $\zeta'_p = \frac{\zeta_p}{\sqrt{\nu\kappa g_J}}$. The above states I_1 and Q_2 can be sent (or prepared at distant) to Bob via remote state preparation (RSP)[4]. Then Bob displaces his mode, i.e. $\alpha_2 = (e^r x_2 + ie^{-r} p_2)/\sqrt{2}$, according to the received signal. In fact, after the measurement the values

Parameter	Symbol	Value
Frequency	ω_i	5 GHz
Measurement bandwidth	B	420 kHz
Resistance	R	50 Ω
HEMT gain	g_H	10^4
Amplification gain of JPA	g_J	10^2
Transfer efficiency (at $T_1=40\text{mK}$)	ϵ	0.95
Transfer efficiency (at $T_2=300\text{K}$, Free space)	η	0.10
Transfer efficiency (at $T_2=4\text{K}$, Fridge)	η	0.90
Transfer efficiency (at $T_3=4\text{K}$)	κ	0.65
Transfer efficiency (at $T_4=100\text{mK}$)	ν	0.75
Local oscillator mode amplitude	$ \alpha_{\text{LO}} $	10^6V/m
Amplification squeezing	r_J	2.30
Squeezing parameter of the TMSS	r	1.32
Transmissivity (for $T_2=300\text{K}$, Free space)	τ	0.095
Transmissivity (for $T_2=4\text{K}$, Fridge)	τ	0.427
Coupling strength (for $T_2=300\text{K}$, Free space)	β	-0.41
Coupling strength (for $T_2=4\text{K}$, Fridge)	β	-2.40
Coefficient (for $T_2=300\text{K}$, Free space)	Λ	1.10
Coefficient (for $T_2=4\text{K}$, Fridge)	Λ	1.74
Noise (zero input, for $T_2=300\text{K}$, Free space)	ζ'_x	$(0.954) \langle I_1 \rangle + (1.152) \langle x_2 \rangle$
Noise (zero input, for $T_2=300\text{K}$, Free space)	ζ'_p	$(0.954) \langle Q_2 \rangle + (0.082) \langle p_2 \rangle$
Noise (zero input, for $T_2=4\text{K}$, Fridge)	ζ'_x	$(0.758) \langle I_1 \rangle + (2.444) \langle x_2 \rangle$
Noise (zero input, for $T_2=4\text{K}$, Fridge)	ζ'_p	$(0.758) \langle Q_2 \rangle + (0.174) \langle p_2 \rangle$

TABLE I. Some approximations for the values in the microwave teleportation circuit

of entangled states already turn to $x_2 = -x_1$ and $p_2 = p_1$. The displacement on Bob's side is implemented with a directional coupler and is described as an asymmetric beam splitter with transmissivity τ , which is $B_S(\tau)_4 = [\sqrt{1-\tau}\mathbb{I}_2, \sqrt{\tau}\mathbb{I}_2; -\sqrt{\tau}\mathbb{I}_2, \sqrt{1-\tau}\mathbb{I}_2]$ with $\tau = 1 - 10^{\beta/10}$, where β is the coupling strength expressed in decibels (dB)[4, 17]. Letting the first moments before the beam splitter as $x_\tau = (I_1, Q_2, e^r x_2, e^{-r} p_2)^T$ by adjusting the parameter τ as

$$\tau = \frac{\epsilon\eta}{2} = 1 - \frac{1}{|\alpha_{\text{LO}}|^2 \hbar\omega_i B R \nu \kappa g_J g_H} \quad (6)$$

and letting $\Lambda = |\alpha_{\text{LO}}|^2 \hbar\omega_i B R \nu \kappa g_J g_H$ therefore $\tau = 1 - \frac{1}{\Lambda}$. Since the maximum value of $\tau = \frac{\epsilon\eta}{2} = 1/2$ then it makes a restriction on Λ as $1 < \Lambda \leq 2$ to have a feasible protocol of teleportation.

The coupling strength turns to

$$\beta = 10 \log \frac{1}{\Lambda} \quad (7)$$

Amplification— The amplification of signals is an essential feature in microwave communication in open air. In the quantum regime, HEMT amplifiers are suited for experiments in the microwave regime. A commercial HEMT usually has $g_H = 10^4$, and working at 5 GHz frequencies it introduces between $n \sim 10 - 100$ thermal photons [17] which can have destructive effects on the proto-

col. Finally, after the operation $B_S(\tau)_4 x_\tau$, the state will be reconstructed in the upper arm after the beam splitter as $\sqrt{2}\alpha_{\text{in}} = e^{-y} x_{\text{in}} + i e^y p_{\text{in}}$ with noise term $\zeta = \zeta'_x + i\zeta'_p$ where the components are

$$\begin{aligned} e^{-y} x_{\text{in}} + \zeta'_x &= \frac{1}{\sqrt{\Lambda}} I_1 + \sqrt{\tau} e^r x_2 \\ e^y p_{\text{in}} + \zeta'_p &= \frac{1}{\sqrt{\Lambda}} Q_2 + \sqrt{\tau} e^{-r} p_2 \end{aligned} \quad (8)$$

In a lossless protocol, $\eta = \epsilon = \kappa = \nu = 1$, the noise term disappears and the state can be reconstructed perfectly, but in reality the amount of loss is significant in the microwave regime. The magnitudes of noise terms ζ'_x and ζ'_p can be obtained experimentally via calibration of the setup by letting the zero input values, i.e. $e^{-y} x_{\text{in}} = 0$ and $e^y p_{\text{in}} = 0$.

col. One alternative for amplification is the replacement of each HMET with two additional JPAs in the same arm (see Fig. 4) to reach the same gain of HEMT but with significant reduction of noise. In this case, the parameter Λ turns to Λ' where $\Lambda'_j = |\alpha_{\text{LO}}|^2 \hbar\omega_i B R \nu \kappa (g_J)^3$ and therefore the state can be reconstructed based on the circuit in Fig. 4, as follows

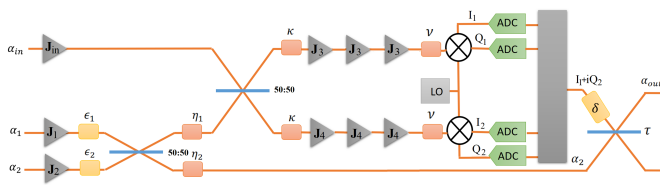


FIG. 4. Replacement of each HEMT with two JPAs in each arm to reach the same gain but with significant lower thermal noise.

$$\begin{aligned}
 e^{-y} x_{\text{in}} + \zeta'_x &= \frac{1}{\sqrt{\Lambda'_J}} I_1 + \sqrt{\tau} e^r x_2 \\
 e^y p_{\text{in}} + \zeta'_p &= \frac{1}{\sqrt{\Lambda'_J}} Q_2 + \sqrt{\tau} e^{-r} p_2
 \end{aligned} \quad (9)$$

ACKNOWLEDGMENTS

The author greatly acknowledges financial support from the projects QMiCS (820505) of the EU Flagship on Quantum Technologies as well as EU project EPIQUS (899368). Also, the author is very grateful for very helpful and constructive discussions with Mikel Sanz, Yasser Omar, Frank Deppe, and Shabir Barzanjeh.

-
- [1] Fedorov, K.G., et al. Displacement of Propagating Squeezed Microwave States. *Phys. Rev. Lett.*, 117, 2, 020502, (2016).
- [2] Goetz, J., et. al. Photon Statistics of Propagating Thermal Microwaves. *Phys. Rev. Lett.*, 118, 10, 103602, (2017).
- [3] Goetz, J., et. al. Second-order decoherence mechanisms of a transmon qubit probed with thermal microwave states. *Quantum Science and Technology*, 2(2), 025002, (2017).
- [4] Pogorzalek, S., et. al. Secure quantum remote state preparation of squeezed microwave states. *Nat. Comm.*, 10, 2604 (2019).
- [5] Sanz, M., Fedorov, K.G., Deppe, F., Solano, E. Challenges in Open-air Microwave Quantum Communication and Sensing. *IEEE Conference on Antenna Measurements & Applications (CAMA)*, 1-4, (2018).
- [6] Fedorov, K.G., et. al. Finite-time quantum entanglement in propagating squeezed microwaves. *Sci. Rep.* 8, 6416 (2018).
- [7] C. Axline et. al. On-demand quantum state transfer and entanglement between remote microwave cavity memories. *Nature Physics*, 14, 705 (2018).
- [8] P. Campagne-Ibarcq et. al. Deterministic Remote Entanglement of Superconducting Circuits through Microwave Two-Photon Transitions. *Phys. Rev. Lett.* 120, 200501, (2018).
- [9] P. Kurpiers et. al. Deterministic quantum state transfer and remote entanglement using microwave photons. *Nature* 558, 264, (2018).
- [10] N. Leung et. al. Deterministic bidirectional communication and remote entanglement generation between superconducting qubits. *npj Quant. Inf.* 5, 18, (2019).
- [11] N. Roch, et. al. Observation of Measurement-Induced Entanglement and Quantum Trajectories of Remote Superconducting Qubits. *Phys. Rev. Lett.* 114, 259901, (2015).
- [12] A. Narla et.al. Robust Concurrent Remote Entanglement Between Two Superconducting Qubits. *Phys. Rev. X*, 6, 031036, (2016).
- [13] C. Dickel et.al. Chip-to-chip entanglement of transmon qubits using engineered measurement fields. *Phys. Rev. B.* 97, 064508, (2018).
- [14] M. Forsch et. al. Microwave-to-optics conversion using a mechanical oscillator in its quantum ground state. *Nature Physics*, 16, 69-74, (2020).
- [15] A. Rueda, et.al. Electro-optic entanglement source for microwave to telecom quantum state transfer. *npj Quantum Information*, 5, 108, (2019).
- [16] P. Magnard, et.al. Microwave Quantum Link between Superconducting Circuits Housed in Spatially Separated Cryogenic Systems. *Phys. Rev. Lett.* 125, 260502 (2020).
- [17] R. Di Candia et al., Quantum teleportation of propagating quantum microwaves. *EPJ Quantum Technology*, 2(1) 25, (2015).
- [18] G. Adesso, S. Ragy, A.R. Lee. Continuous Variable Quantum Information: Gaussian States and Beyond. *Open Syst. Inf. Dyn.* 21, 1440001 (2014).
- [19] Adesso, G., and F. Illuminati, Entanglement in continuous-variable systems: recent advances and current perspectives. *J. Phys. A: Math. Theor.* 40, 7821 (2007).
- [20] Weedbrook C, et. al., Gaussian quantum information. *Rev. Mod. Phys.* 84, 621 (2012).
- [21] A. Ferraro, S. Olivares, M.G.A. Paris, Gaussian states in continuous variable quantum information. *arXiv preprint: quant-ph/0503237* (2005).
- [22] A. Serafini. *Quantum Continuous Variables*. CRC Press, Taylor & Francis Group, LLC (2017).
- [23] L. Vaidman, Teleportation of quantum states. *Phys. Rev. A* 49, 1473 (1994).
- [24] S.L. Braunstein and H.J. Kimble, Teleportation of Continuous Quantum Variables. *Phys. Rev. Lett.* 80, 869 (1998).
- [25] A. Furusawa et.al. Unconditional Quantum Teleportation. *Science*, 282, 706-709, (1998).
- [26] Pirandola, S., and S. Mancini, Quantum teleportation with continuous variables: A survey. *Laser Physics* 16, 1418 (2006).
- [27] Braunstein, S. L., and P. van Loock, Quantum information with continuous variables. *Rev. Mod. Phys.* 77, 513 (2005).

- [28] J.I. Cirac, P. Zoller, H. J. Kimble, and H. Mabuchi, Quantum State Transfer and Entanglement Distribution among Distant Nodes in a Quantum Network. *Phys. Rev. Lett.* **78**, 3221 (1997).
- [29] A. A. Clerk, M. H. Devoret, S. M. Girvin, F. Marquardt, and R. J. Schoelkopf, Introduction to quantum noise, measurement, and amplification. *Rev. Mod. Phys.* **82**, 1155 (2010).
- [30] Aoki, T., G. Takahashi, T. Kajiya, J. Yoshikawa, S. L. Braunstein, P. van Loock, and A. Furusawa, Quantum error correction beyond qubits. *Nature Physics* **5**, 541 (2009).
- [31] S. Pirandola, Satellite Quantum Communications: Fundamental Bounds and Practical Security. arXiv: 2012.01725 (2020).

Appendix A: Continuous Variables and Gaussian States

In quantum mechanics, a continuous variable (CV) system is defined as a system with degrees of freedom associated to operators with a continuous spectrum, whose eigenstates form bases for the infinite-dimensional Hilbert space \mathbb{H} . For example, a quantized electromagnetic field is a bosonic CV system that can be modeled as a collection of non-interacting quantum harmonic oscillators with different frequencies, where each oscillator is referred to as a mode of the system [18, 19]. CV systems are represented by N bosonic modes with an infinite-dimensional Hilbert space $\mathbb{H}^{\otimes N} = \otimes_{k=1}^N \mathbb{H}_k$, corresponding to N quantum harmonic oscillators associated with N pairs of annihilation and creation operators $\{a_k, a_k^\dagger\}_{k=1}^N$, respectively, which can be sorted in a vectorial operator $\hat{l} = (\hat{a}_1, \hat{a}_1^\dagger, \dots, \hat{a}_N, \hat{a}_N^\dagger)$, satisfying in the bosonic commutation relations $[\hat{l}_i, \hat{l}_j] = \Omega_{ij}$, $i, j = 1, \dots, 2N$ where Ω_{ij} is the generic element of $2N \times 2N$ matrix $\Omega := \oplus_{k=1}^N \omega$, $\omega := \begin{pmatrix} 0 & 1 \\ -1 & 0 \end{pmatrix}$ known as the symplectic form [18]. Besides $\{a_k, a_k^\dagger\}$ operators, a bosonic system may be described by the quadrature field operators $\{q_k, p_k\}_{k=1}^N$, sorted in the vector $\hat{x} = (\hat{q}_1, \hat{p}_1, \dots, \hat{q}_N, \hat{p}_N)$, which are associated to the bosonic field operators via $\hat{a}_k := \frac{1}{\sqrt{2}}(\hat{q}_k + i\hat{p}_k)$. The quadrature field operators act like the position and momentum operators of the quantum harmonic oscillator, satisfying in the canonical commutation relations in natural units ($\hbar = 2$), $[\hat{x}_i, \hat{x}_j] = 2i\Omega_{ij}$. The N -mode Hilbert space can be written as $\hat{x}^T|x\rangle = x^T|x\rangle$ with $x \in \mathbb{R}^{2N}$ and $|x\rangle := (|x_1\rangle, \dots, |x_{2N}\rangle)^T$. A quantum state represented by a density operator $\hat{\rho}$ includes all the physical information about the N -mode bosonic system, which has an equivalent representation in terms of a quasi-probability distribution, i.e. Wigner function, over a real phase space. Also, it is equivalent to a Wigner characteristic function $\chi(\xi) = \text{tr}[\hat{\rho}D(\xi)]$ where $D(\xi) := \exp(i\hat{x}^T\Omega\xi)$ is the Weyl operator with $\xi \in \mathbb{R}^{2N}$ that can be converted to a Wigner function via Fourier transform $W(x) = \int_{\mathbb{R}^{2N}} \frac{d^{2N}\xi}{(2\pi)^{2N}} \exp(-ix^T\Omega\xi)\chi(\xi)$, i.e. normalized to one but non-positive quasiprobability distribution in

general [18, 20]. The CVs, $x \in \mathbb{R}^{2N}$, which are the eigenvalues of quadratures operator \hat{x} , span a real symplectic space $(\mathbb{R}^{2N}, \Omega)$, in which a N -mode bosonic state ρ is equivalent to a Wigner function $W(x)$ defined over a $2N$ -dimensional phase space. The statistical moments of the quantum state characterize χ or W where the first moment is called the displacement vector or the mean value $\bar{x} := \langle \hat{x} \rangle = \text{tr}(\hat{x}\rho)$, and the second moment is called the covariance matrix V , i.e. a $2N \times 2N$, real and symmetric matrix, with elements $V_{ij} := \frac{1}{2}\{\{\Delta\hat{x}_i, \Delta\hat{x}_j\}\}$ where $\Delta\hat{x}_i := \hat{x}_i - \langle \hat{x}_i \rangle$ and $\{\cdot, \cdot\}$ is the anti-commutator. In fact, the diagonal elements of the covariance matrix are the variances of the quadrature operators, i.e., $V_{ii} = V(\hat{x}_i)$ where $V(\hat{x}_i) = \langle (\Delta\hat{x}_i)^2 \rangle = \langle \hat{x}_i^2 \rangle - \langle \hat{x}_i \rangle^2$. The covariance matrix must satisfy the uncertainty principle $V - i\Omega \geq 0$, implying the positive definiteness $V > 0$. The first two moments are sufficient for a complete characterization, i.e. $\hat{\rho} = \hat{\rho}(\bar{x}, V)$, which is used for the case of Gaussian states that are bosonic states with Gaussian Wigner representation (χ or W). In classical physics, Gaussian functions are mostly introduced in probability theory, often under the name of “normal distributions”, but in quantum theory, Gaussian states are very closely related to Gaussian functions, which are defined as states whose characteristic functions and quasiprobability distributions are Gaussian functions on the quantum phase space [18]. In fact, a pure state is Gaussian, if and only if, its Wigner function is non-negative, and one can obtain the Wigner function of each Gaussian state by letting its covariance matrix in the formula $W(x) = \frac{\exp\{-1/2((x-\bar{x})^T V^{-1}(x-\bar{x}))\}}{(2\pi)^N \sqrt{\det V}}$ [20]. Furthermore, a quantum operation is named Gaussian when it preserves the nature of a Gaussian state. Thus, Gaussian channels (unitaries) are those channels which preserve the Gaussian character of a quantum state. Gaussian unitaries are generated via $S = \exp(-i\hat{H}/2)$ from Hamiltonians \hat{H} which are second-order polynomials in the field operators. In terms of the quadrature operators, a Gaussian unitary is more simply described by map $(S, d) : \hat{x} \rightarrow S\hat{x} + d$ where $d \in \mathbb{R}^{2N}$ and S is a $2N \times 2N$ real matrix, and it is symplectic if it satisfies in $S\Omega S^T = \Omega$. It can be shown that, if S , S_1 and S_2 are symplectic, then S^{-1} , S^T and $S_1 S_2$ are also symplectic [21], with $S^{-1} = \Omega S^T \Omega^{-1}$. The action of a Gaussian unitary in terms of the statistical moments, \bar{x} and V , is [20, 21]

$$\bar{x} \rightarrow S\bar{x} + d, \quad V \rightarrow SVS^T. \quad (\text{A1})$$

In this paper, our notations are mostly in symplectic representation in terms of statistical moments.

Appendix B: Single- and Two-mode Gaussian States

In this paper, we have only considered single-mode ($N = 1$) and two-mode ($N = 2$) Gaussian states to be used in the teleportation protocol, which will be discussed in the following sections. Now, we show the covariance matrix representation of single-mode Gaussian

states, V_G , as states to be processed, transferred and measured. In the following sections, $\mathbb{I}_2 = \begin{pmatrix} 1 & 0 \\ 0 & 1 \end{pmatrix}$ will describe the 2×2 identity matrix. One can show that any 2×2 symplectic matrix, as a single-mode Gaussian state with mean \bar{x} and covariance matrix V_G , is in its most general form as $V_G = (2n+1)R(\theta)S(2r)R(\theta)^T$ [20]. Single mode Gaussian states comprise vacuum states ($\bar{x} = 0$), $V_0 = \mathbb{I}_2$, coherent states ($\bar{x} \neq 0$), $V_c = \mathbb{I}_2$, thermal states $V_{th} = (2n+1)\mathbb{I}_2$, squeezed vacuum states ($\bar{x}=0$) and squeezed coherent states ($\bar{x} \neq 0$). These two have the same covariance matrices, $V_r = \begin{pmatrix} e^{-2r} & 0 \\ 0 & e^{2r} \end{pmatrix}$ and $V_{-r} = \begin{pmatrix} e^{2r} & 0 \\ 0 & e^{-2r} \end{pmatrix}$, where r is the squeezing level, n is the number of thermal photons. A rotation matrix is $R(\theta) = \begin{pmatrix} \cos \theta & \sin \theta \\ -\sin \theta & \cos \theta \end{pmatrix}$, where θ is the angle of rotation and $S(r) = \begin{pmatrix} e^{-r} & 0 \\ 0 & e^r \end{pmatrix}$ is the squeezing matrix. Then, the covariance matrix V_r is obtained as $V_r = S(r)S(r)^T = S(2r) = \begin{pmatrix} e^{-2r} & 0 \\ 0 & e^{2r} \end{pmatrix}$ that has different quadrature noise-variances, i.e., one variance is squeezed below the quantum shot-noise, while the other is anti-squeezed above it.

Gaussian states of two bosonic modes ($N=2$) are characterized by simple analytical formulas, which makes them the simplest states for studying properties like quantum entanglement. The covariance matrix of a two-mode Gaussian (TMG) state in symplectic representation is shown by a block matrix as follows [22], $V_{TMG} = [A, C; C^T, B]$, where $A = A^T$, $B = B^T$ and C is a 2×2 real matrix. Two-mode squeezed states (TMSS) are the most useful TMG states in quantum information protocols where entanglement sharing between two parties are required. The two-mode squeezing operator as a Gaussian unitary is defined as $\hat{S}_2(r) = \exp[r(\hat{a}\hat{b} - \hat{a}^\dagger\hat{b}^\dagger)]$. By applying $\hat{S}_2(r)$ to a couple of vacuum states $|0\rangle_a|0\rangle_b$, we obtain the two-mode squeezed vacuum (TMSV) state, $|\lambda\rangle = \sqrt{1-\lambda^2} \sum_{n=0}^{\infty} (-\lambda)^n |n\rangle_a |n\rangle_b$ where $\lambda = \tanh(r) \in [0, 1]$ [20]. In symplectic representation, TMSV state are characterized by $A = B = \cosh(2r)\mathbb{I}_2$ and $C = \sinh(2r)\mathbb{Z}$ with $\mathbb{Z} = \text{diag}(1, -1)$. The symmetric two-mode squeezed thermal state (TMST) can be expressed by $A = B = (2n+1)\cosh(2r)\mathbb{I}_2$ and $C = (2n+1)\sinh(2r)\mathbb{Z}$ with equal number of thermal photons, n , in each mode. Normally, TMSV and TMST states are the most useful Gaussian resources in quantum protocols, e.g. in quantum teleportation.

The Wigner function of TMG states can be obtained by replacing V by V_{TMG} in the formula of $W(x)$, where x turns to $x = (x_1 \ p_1 \ x_2 \ p_2)^T$.

1. Measurement in Teleportation of Gaussian States

The Braunstein-Kimble protocol describes a CV teleportation procedure with quantum states employing Gaussian resources [24]. Let us consider a situation in which two parties, Alice and Bob, want to share a TMSS.

Then, Alice tries to send a single-mode Gaussian state to Bob via the teleportation mechanism. Alice performs double homodyne detection (see Fig. 2), which is the optimal measurement for the teleportation protocol. In this case, the result of the measurement will be modulated as a single mode δ to be sent to Bob. As can be seen in Fig. 2, two modes α_{in} and α_1 are passing through a 50:50 beamsplitter, and then again each output beam again passes through two other 50:50 beamsplitters while a classical local oscillator mode α_{LO_x} enters in the top beamsplitter and another classical local oscillator mode α_{LO_p} passes through the other beamsplitter. According to Fig. 2 in each line for quantum modes we use the annihilation operators, and α as classical coherent state for the local oscillator. Finally, there would be four outputs at the end, where there is a detector at each output which can measure the current produced due to the collision of photons to the detector.

In the symplectic representation, we consider two operators in the double-homodyne detection circuit depicted in Fig. 2, $S_{h1} = \mathbb{I}_2 \oplus B_S(1/2)_4 \oplus \mathbb{I}_2$ and $S_{h2} = B_S(1/2)_4 \oplus B_S(1/2)_4$. The input first moment in the double-homodyne detection is $x'_{in} = (x_{LO_x}, p_{LO_x}, x_{in}, p_{in}, e^r x_1, e^{-r} p_1, x_{LO_p}, p_{LO_p})^T$, and therefore the output's first moments at the photodetectors right before the measurement are $x'_{out} = S_{h2}S_{h1}x'_{in}$, which gives $x'_{out} = \sqrt{2}((x_{u'}), (p_{u'}), (x_{u''}), (p_{u''}), (x_{v'}), (p_{v'}), (x_{v''}), (p_{v''}))^T$ where $\text{Re}(\alpha_{u'}) = x_{u'} = 1/2(x_{in} + e^r x_1) + x_{LO_x}/\sqrt{2}$, $\text{Im}(\alpha_{u'}) = p_{u'} = 1/2(p_{in} + e^{-r} p_1) + p_{LO_x}/\sqrt{2}$, $\text{Re}(\alpha_{u''}) = x_{u''} = 1/2(x_{in} + e^r x_1) - x_{LO_x}/\sqrt{2}$, $\text{Im}(\alpha_{u''}) = p_{u''} = 1/2(p_{in} + e^{-r} p_1) - p_{LO_x}/\sqrt{2}$, $\text{Re}(\alpha_{v'}) = x_{v'} = 1/2(-x_{in} + e^r x_1) + x_{LO_x}/\sqrt{2}$, $\text{Im}(\alpha_{v'}) = p_{v'} = 1/2(-p_{in} + e^{-r} p_1) + p_{LO_x}/\sqrt{2}$, $\text{Re}(\alpha_{v''}) = x_{v''} = 1/2(x_{in} - e^r x_1) + x_{LO_x}/\sqrt{2}$, and $\text{Im}(\alpha_{v''}) = p_{v''} = 1/2(p_{in} - e^{-r} p_1) + p_{LO_x}/\sqrt{2}$. Here, we assume that the detectors are ideal, therefore we define the produced current as $i = \langle \hat{n} \rangle = \langle \hat{a}^\dagger \hat{a} \rangle = \langle 1/2(\hat{x}^2 + \hat{p}^2) - 1/2 \rangle = 1/2(x^2 + p^2) - 1/2$. Then, the difference between the currents from each detector after the beam splitters is measured [27]. The current from the top beamsplitter is the difference between the currents in u' and u'' , i.e. $i_1 = \langle \hat{a}_{u'}^\dagger \hat{a}_{u'} \rangle - \langle \hat{a}_{u''}^\dagger \hat{a}_{u''} \rangle$, which gives $i_1 = \frac{1}{\sqrt{2}}[(x_{in} + e^r x_1)x_{LO_x} + (p_{in} + e^{-r} p_1)p_{LO_x}]$. Assuming $\alpha_{LO_x} = |\alpha_{LO_x}\rangle e^{i\theta_x} = |\alpha_{LO_x}\rangle (\cos \theta_x + i \sin \theta_x)$, and equivalently $\alpha_{LO_x} = \frac{(x_{LO_x} + ip_{LO_x})}{\sqrt{2}}$, if $\theta_x = 0$ then $x_{LO_x} = \sqrt{2}|\alpha_{LO_x}|$ and $p_{LO_x} = 0$, thus $i_1 = |\alpha_{LO_x}|(x_{in} + e^r x_1)$ that consequently one can obtain $X_u = \frac{i_1}{|\alpha_{LO_x}|} = x_{in} + e^r x_1 = \text{Re}(\delta)$. Similarly, in the other two arms the current difference is $i_2 = \langle \hat{a}_{v'}^\dagger \hat{a}_{v'} \rangle - \langle \hat{a}_{v''}^\dagger \hat{a}_{v''} \rangle$ yields $i_2 = \frac{1}{\sqrt{2}}[(x_{in} - e^r x_1)x_{LO_x} + (p_{in} - e^{-r} p_1)p_{LO_x}]$. Assuming $\alpha_{LO_p} = |\alpha_{LO_p}\rangle e^{i\theta_p}$, if we let $\theta_p = \pi/2$ then it turns to $i_2 = |\alpha_{LO_p}|(p_{in} - e^{-r} p_1)$, and therefore $P_v = \frac{i_2}{|\alpha_{LO_p}|} = p_{in} - e^{-r} p_1 = \text{Im}(\delta)$. By using classical coherent light with similar amplitudes for both local

oscillators, one can write $|\alpha_{LO_x}\rangle = |\alpha_{LO_p}\rangle = |\alpha_{LO}\rangle$, so the currents i_1 and i_2 can be modulated into a single mode as $\delta = X_u + iP_v$, to be sent and received by Bob (see Fig. 2). On the other side, at the same time that Alice measures her state, the state at Bob collapses to $\alpha_2 = \frac{e^r x_2 + i e^{-r} p_2}{\sqrt{2}}$ with $x_2 = -x_1$ and $p_2 = p_1$. The goal of teleportation is to reconstruct $\alpha_{in} = \frac{x_{in} + i p_{in}}{\sqrt{2}}$ from the received state $\delta = \frac{(x_{in} + e^r x_1) + i(p_{in} - e^{-r} p_1)}{\sqrt{2}}$ and $\alpha_2 = \frac{-e^r x_1 + i e^{-r} p_1}{\sqrt{2}}$. Comparing δ and α_2 we realize that $\delta + \alpha_2 = \alpha_{in}$ where δ is the complex conjugate of δ . Once Bob receives this information, he can reconstruct Alice's input state by applying the displacement $D(\delta)$ on his mode, i.e. $D(\delta)|\alpha_2\rangle = |\delta + \alpha_2\rangle = |\alpha_{out}\rangle \approx |\alpha_{in}\rangle$. In the symplectic representation, this means that the first moments of Bob, $\bar{x}_2 = (x_2, p_2)^T$ should be displaced with $\Delta = (X_u, P_v)^T$, which means

$$\bar{x}_2 \rightarrow \bar{x}_2 + \Delta. \quad (B1)$$

2. Fidelity of Teleportation in Free Space

In order to obtain the fidelity in free space, we consider that the resource is a TMSV state interacting in free space with a thermal bath characterized by N thermal photons. This mechanism is modeled via a beamsplitter with reflectivity η , i.e. $B_S(\eta)$. In Fig. 5a in the circuit $\mathbf{V}'_{out} = S'_1 V'_{in} S'^T_1$ where the input is $V'_{in} = (2N+1)\mathbb{I}_2 \oplus V_{TMSV}$ with N as the number of environmental thermal photons, and $\mathbf{S}'_1 = B_S(\eta)_4 \oplus \mathbb{I}_2$, thus the output covariance matrix in block form is $V'_{out} = [A', C'; C', B']$, where $A' = [(2N+1)(1-\eta) + \eta \cosh(2r)]\mathbb{I}_2$, $B' = \cosh(2r)\mathbb{I}_2$, and $C' = \sqrt{\eta} \sinh(2r)\mathbb{Z}$. This interaction between a TMSV state with squeezing level r and a thermal bath with N thermal photons in free space can be modeled by a two-mode squeezed thermal (TMST) state with n thermal photons in the resource and squeezing level s' . In this case, we use the local operations L_1 and L_2 in the circuit (see Fig. 5) to obtain the parameters of (TMSV state + Air) in terms of TMST state. Then, we obtain $V''_{out} = S'_2 V_{TMST} S'^T_2$, where $S'_2 = L_1 \oplus L_2$

$$\begin{aligned} s' &= \frac{1}{2} \tanh^{-1} \left(\frac{\sqrt{\eta} \sinh(2r)}{(1-\eta)(2N+1) + \eta \cosh(2r)} \right), \\ x_1 &= \frac{1}{8} \log(\operatorname{sech}(2r)(-\eta - 2\eta N + 2N + \eta \cosh(2r) + 1)), \\ x_2 &= -\frac{3}{8} \log(\operatorname{sech}(2r)(-\eta - 2\eta N + 2N + \eta \cosh(2r) + 1)), \\ n &= \frac{1}{2} \left(\sqrt{\operatorname{sech}(2r)((\eta-1)(-2N-1) + \eta \cosh(2r)) \left(((\eta-1)(2N+1) - \eta \cosh(2r))^2 - \eta \sinh^2(2r) \right)} - 1 \right). \end{aligned} \quad (B3)$$

The term under the radical makes a restriction on the

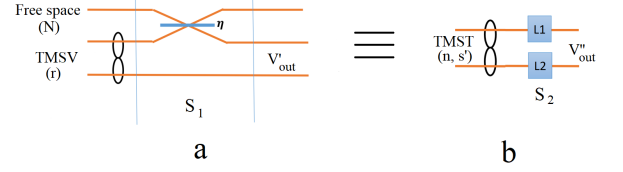


FIG. 5. a) The interaction model of TMSV state with squeezing level r with free space including N thermal photons via a beamsplitter with reflectivity η , and b) The operation of local operations L_1 and L_2 on the TMST state with squeezing level s'

After the local operations (which are squeezing operators. L_1 with squeezing x_1 and L_2 with squeezing x_2)

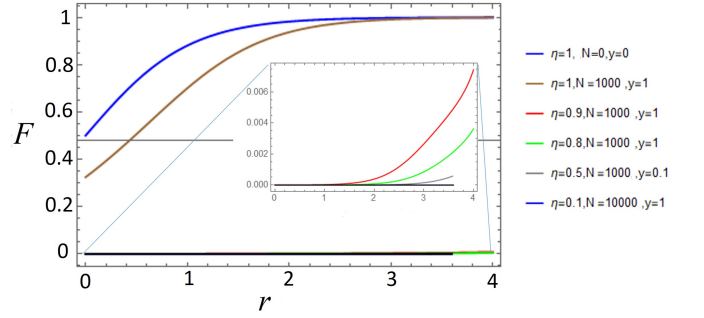


FIG. 6. Teleportation fidelity of Gaussian states in free space in terms of TMSV squeezing level r for different values of air thermal photons N and beamsplitter reflectivity η (i.e. efficiency of transfer) for different squeezing level of the input y .

we have $V''_{out} = [A'', C''; C'', B'']$, where the matrices A'' , B'' , and C'' are

$$\begin{aligned} A'' &= [e^{-4x_1}(2n+1) \cosh(2s'), 0; 0, e^{4x_1}(2n+1) \cosh(2s')], \\ B'' &= [e^{-4x_2}(2n+1) \cosh(2s'), 0; 0, e^{4x_2}(2n+1) \cosh(2s')], \\ C'' &= [e^{-2(x_1+x_2)}(2n+1) \sinh(2s'), 0; 0, -e^{2(x_1+x_2)}(2n+1) \sinh(2s')]. \end{aligned} \quad (B4)$$

If we equal V'_{out} to V''_{out} , we find

squeezing level which should satisfy

$$1 - \frac{\eta \sinh^2(2r)}{((\eta-1)(2N+1) - \eta \cosh(2r))^2} > 0. \quad (B4)$$

The fidelity is obtained via $F = 2/\sqrt{\det(\Gamma)}$, in which $\Gamma = 2V_{\text{in}}' + \mathbb{Z}A''\mathbb{Z} + B'' - C''\mathbb{Z} - \mathbb{Z}^T C''^T$ where A'' , B'' , and C'' are the block matrices of $V_{\text{out}}'' = [A'', C''; C''^T, B'']$.

The diagram of the fidelity in terms of r , for different

values of η and N , and for different squeezing level y of input states has been shown in Fig. 6. It can be seen that the fidelity is affected significantly by variations in η and N . To be quantum teleportation, the fidelity should be higher than 0.50, otherwise the protocol is classical.